

CALIFORNIA STATE UNIVERSITY, NORTHRIDGE

PROTEIN FOLDING: PLANAR CONFIGURATION SPACES OF DISC  
ARRANGEMENTS AND HINGED POLYGONS

A thesis submitted in partial fulfillment of the requirements for the degree of  
Master of Science in Applied Mathematics

by

Clinton Bowen

August 2014

The thesis of Clinton Bowen is approved:

---

Dr. Silvia Fernandez

---

Date

---

Dr. John Dye

---

Date

---

Dr. Csaba Tóth, Chair

---

Date

California State University, Northridge

## Table of Contents

<b>Signature page</b> . . . . .	<b>ii</b>
<b>Abstract</b> . . . . .	<b>iv</b>
 <b>Chapter 1</b>	
<b>Realizability of Polygonal Linkages with Fixed Orientation</b> . . . . .	<b>1</b>
1.1 Auxiliary Construction . . . . .	2
1.1.1 Functionality of the Auxiliary Construction and Gadgets . . . . .	8
 <b>Chapter 2</b>	
<b>Realizability Problems for Weighted Trees</b> . . . . .	<b>21</b>
2.1 Properties for Weighted Trees and Polygonal Linkages . . . . .	21
2.2 Approximating Regular Hexagons with Snowflakes . . . . .	21
2.3 On the Decidability of Problem ?? . . . . .	25

ABSTRACT

PROTEIN FOLDING: PLANAR CONFIGURATION SPACES OF DISC ARRANGEMENTS AND

HINGED POLYGONS

By

Clinton Bowen

Master of Science in Applied Mathematics

## Chapter 1

### Realizability of Polygonal Linkages with Fixed Orientation

We begin the chapter with describing several gadgets that translates the associated graph  $A(\Phi)$  of a P3SAT boolean formula. These gadgets will be used together to form a special hexagonal tiling that behaves in a similar nature to the logic engine that encoded a NAE3SAT instance of Chapter ?? but instead encodes a Planar 3-SAT and its associated graph. Together the gadgets will form what is called the auxiliary construction. The hexagonal tiling would then be used to prove the following theorem:

**Theorem 1.** *It is strongly NP-hard to decide whether a polygonal linkage whose hinge graph is a **tree** can be realized with counter-clockwise orientation.*

Our proof is a reduction from P3SAT. Given an instance  $\Phi$  of P3SAT with  $n$  variables and  $m$  clauses and its associated graph  $A(\Phi)$ , we construct a simply connected polygonal linkage  $(\mathcal{P}, H)$ , of polynomial size in  $n$  and  $m$ , such that  $\Phi$  is satisfiable if and only if  $(\mathcal{P}, H)$  admits a realization with fixed orientation.

We construct a polygonal linkage in two main steps: first, we construct an auxiliary structure where some of the polygons have fixed position in the plane (called *obstacles*), while other polygons are flexible, and each flexible polygon is hinged to an obstacle. Second, we modify the auxiliary construction into a polygonal linkage by allowing the obstacles to move freely, and by adding new polygons and hinges as well as an exterior *frame* that holds the obstacle polygons in place. All polygons in our constructions are regular hexagons or long, skinny rhombi because these are the polygons that we can “simulate” with disk arrangements in Chapter 2.

Here is a glossary of important formulas for this chapter:

$z(n, m)$	$=$	$4s(n, m)$
$J_h(z)$	$=$	$6z(n, m) + 1 = 24s(n, m) + 1$
$J_d(z)$	$=$	$4z(n, m) + 1 = 16s(n, m) + 1$
$N(n, m)$	$=$	$\dots =$
$t(n, m)$	$=$	$2N^3(n, m) - 1 =$
$H(n, m)$	$=$	$(12s + 1)2s\sqrt{3} + 12s\left(\frac{1}{100N} + \sqrt{3}\right) =$

**Modifying the Associated Graph of a P3SAT.** Given an instance of P3SAT boolean formula  $\Phi$  of  $n$  variables and  $m$  clauses with associated graph  $A(\Phi)$ , we construct a finite *honeycomb* grid  $H_{A(\Phi)}$  of regular hexagons over the plane centered at origin. We modify the associated graph drawing  $A(\Phi)$  by overlaying it onto a honeycomb in the following way:

1. **Variable:** A vertex representing a variable shall encompass a consecutive set of hexagons along a horizontal line in the honeycomb (see Figure 1.1).

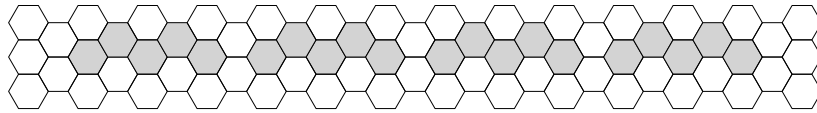


Figure 1.1: The four shaded groups of horizontally adjacent hexagons represent four distinct variables from a boolean formula in the honeycomb.

Let  $D = \max_{v \in V} \deg(v)$  where  $V$  is the set of vertices of  $A(\Phi)$ . Every variable vertex  $v$  must encompass at least  $2 \cdot \deg(v)$  consecutive hexagons but can encompass upto  $2 \cdot D$  consecutive hexagons.

2. **Clause:** A vertex representing a clause shall be a vertex of a hexagon in the honeycomb.
3. **Edge:** Edges of the associated graph  $A(\Phi)$  are paths between the variable  $x_i$  and clause  $C_j$ . An edge  $\{x_i, C_j\}$  of the associated graph is pairwise edge disjoint. The edges of the drawing shall traverse the edges of hexagons in a vertically or horizontally zigzagging manner (see Figure 1.2) in the honeycomb from the literal to the corresponding clause. Edges traverse a hexagon in two edges vertically, three edges horizontally. The vertical zigzagging edge segments traverse the left or right sides of a hexagon(s). The horizontal zigzagging edge segments traverse the top or bottom halves of a hexagon(s). When the edge transitions from a vertical to horizontal traversal, the edge traverses in over 4 edges about the hexagon. The length of the edges are bounded above by  $6 \cdot (\ell_1(x_i, C_j) + D)$  where  $\ell_1$  is the  $L_1$  norm.

It was shown that if  $G = (V, E)$  is planar, it can be embedded in an  $|V| \times |V|$  grid with  $2.4|V| + 4$  bends [1, 2]. From this result, we can define the side length polynomial  $s(n, m)$  to account for the hexagons in the grid and let  $s(n, m)$  to be something greater than  $2.4(n + m) + 4$ , e.g.:

$$6(n + m) + 4.$$

Figure 1.2 illustrates an associated graph of a P3SAT overlaid on a honeycomb. This type of construction emulates an *orthogonal drawing* over a hexagonal grid; an orthogonal drawing where edges are drawn with alternating vertical and horizontal line segments. Let the region in which the construction lies in be a regular hexagon region with polynomial side length  $s(n, m)$ .

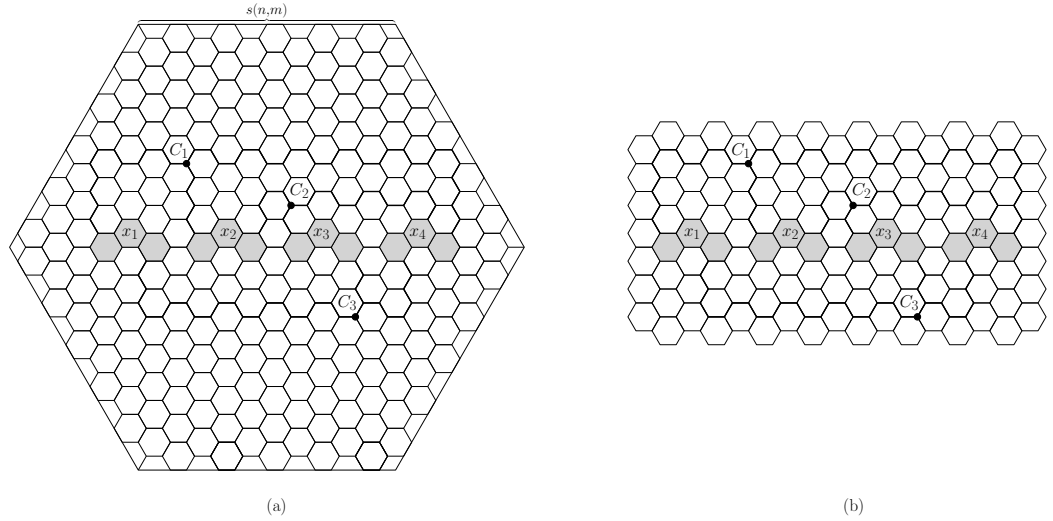


Figure 1.2: (a) This is an instance of an associated graph for a P3SAT overlaid onto a honeycomb grid and placed into a regular hexagonal region of sidelength  $s(n, m)$ . This honeycomb graph could correspond to Boolean formula  $(\neg x_1 \vee \neg x_2 \vee x_4) \wedge (x_2 \vee \neg x_3 \vee x_4) \wedge (x_1 \vee \neg x_3 \vee \neg x_4)$ . (b) This is the same instance as (a) shown without the hexagonal region.

The honeycomb construction will act as preliminary concept that will be refined further in the Auxiliary Construction. The polynomial  $s(n, m)$  will be used to construct the gadgets for the construction.

### 1.1 Auxiliary Construction

Let  $\Phi$  be a Boolean formula of P3SAT with variables  $x_1, \dots, x_n$  and clauses  $C_1, \dots, C_m$ , where  $A(\Phi)$  is the associated planar graph and  $\hat{A}(\Phi)$  be corresponding honeycomb graph. We continue to modify  $\hat{A}(\Phi)$  to form the auxiliary construction. Consider a large (polynomial-size) regular hexagon  $J$  with side length  $s(n, m)$  that contains all gadgets in our construction and hexagonal grid. For each hexagon of the hexagonal grid

contained in  $J$ , scale the hexagon in the following way: first we fix the center of the hexagon and then scale (shrink) the hexagon; adjacent hexagons in the honeycomb no longer touch each other and form corridors and junctions between the hexagons (See Figure 1.3).

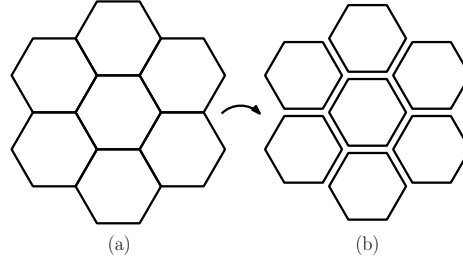


Figure 1.3: (a) This figure shows a region of a hexagonal grid scaled in place to form corridors between adjacent hexagons (shown in (b)).

Formally, let a *corridor* be a channel between two adjacent hexagons and a *junction* be a region where three corridors meet.

**Formal Description of the Auxiliary Construction.** Given the side length of  $J$ ,  $s(n, m)$ , we need to scale the grid of hexagons of the hexagonal grid in the interior of  $J$  accordingly.

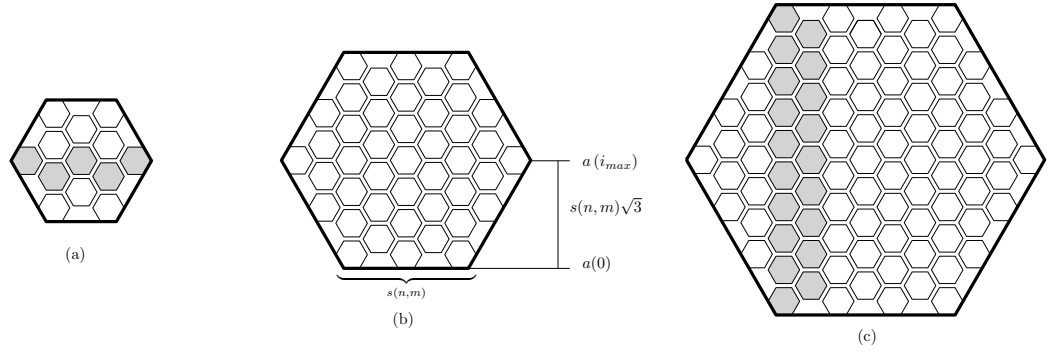


Figure 1.4: (a) shows a *formal auxiliary construction* with  $k = 2$ .  $k$  is the number of hexagons of the hexagonal grid in the interior of  $J$  that is on the bottom most row. (b) shows a formal auxiliary construction with  $k = 3$ . (c) shows a formal auxiliary construction with  $k = 4$ . Note that in each figure

In Figure 1.4, we show the three smallest possible formal constructions of  $J$ ,  $J_1, J_2, J_3$ . A *formal construction* of  $J$  is when six hexagons of the hexagonal grid each have two adjacent sides on the perimeter of  $J$ . We have shown informal constructions earlier where this does not occur. Unless otherwise specified, we will assume the use of formal constructions. Each of the figures in Figure 1.4 shows  $J$  in bold and the hexagonal grid in its interior. Notice that in each case we have six hexagons of the hexagonal grid with each of the six hexagons having two adjacent sides that lie on the perimeter of  $J$ .

The height and diameter of  $J$  can be described by the number of hexagons in the grid a vertical or horizontal line may cross. We'll denote these qualities as the hexagonal height and hexagonal diameter of  $J$ . Figure 1.4(c) and Figure 1.4(a) show the hexagonal height and hexagonal diameters of  $J_1$  and  $J_3$  respectively. The formula for calculating hexagonal height of  $J_z$  is

$$J_h(z) = 6z + 1 \quad (1.1)$$

The formula for calculating the hexagonal diameter of  $J_z$  is

$$J_d(z) = 4z + 1 \quad (1.2)$$

If an associated graph of a P3SAT instance can be encoded into a honeycomb grid of size  $s(n, m) \times s(n, m)$ , then let  $z(n, m) = 4 \cdot s(n, m)$  to enclose the same honeycomb to be enclosed into the interior of  $J_z$ .

Figure 1.4(b) illustrates the side length of  $J$  as  $s(n, m)$  and half the height of  $J$  as  $s(n, m)\sqrt{3}$ . For any  $J$ , there is a fixed number of hexagons in the hexagonal grid that lie on one side of the perimeter of  $J$ ; denote this number as  $k$ . We can denote the number of hexagons in a row of the hexagonal grid in  $J_z$  with the following sequence as follows:

$$\begin{aligned} a(0) &= k \\ a(1) &= k - 1 \\ a(2) &= k \\ a(i) &= a(i - 3) + 1 \\ 0 \leq i &\leq \left\lceil \frac{J_h(z)}{2} \right\rceil \end{aligned} \tag{1.3}$$

The  $i^{\text{th}}$  number of Sequence 1.3 indicates the number of hexagons on the  $i^{\text{th}}$  row of the hexagonal grid in the interior of  $J$  from the perimeter of  $J$  up to the half height of  $J$ . In Figure 1.4(c) from the bottom to the mid-height of  $J$ , the sequence  $a(i)$  (i.e. the number of hexagons in each subsequent row) is 4, 3, 4, 5, 4, 5, 6, 5, 6, 7.

Denote the hexagons of the hexagonal grid in  $J$  as *obstacle hexagons*. Let the side length of the an obstacle hexagon be  $N(n, m) = c_N \cdot s(n, m)$  where  $c_N \in (0, \frac{1}{2z+1})$ . The scaling constant  $c_N$  preserves the corridors described described earlier.

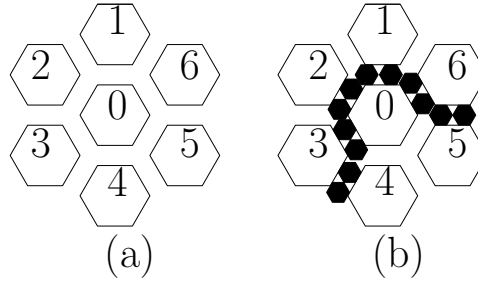


Figure 1.5: (a) A region of the honeycomb shown with scaling. The corridors and junctions formed from the first scaling is preserved after scaling the honeycomb grid to where the side lengths of the hexagon are  $N(n, m)$ . (b) The same region in (a) containing flags.

Let the numbered hexagons of Figure 1.5(a) be obstacle hexagons that are fixed. In Figure 1.5(b), we have smaller hexagons within some corridors and junctions. These hexagons are flags. For each edge in  $\tilde{A}(\Phi)$ , we insert flags into the corridor corresponding to that edge. Flexible hexagons are hinged at the vertex closest to origin and the side of the corridor (See Figure 1.6). Let  $t(n, m) = 2N^3(n, m) - 1$  be the number of flags in a corridor (see Figure 1.6). Scale the honeycomb such that the obstacle hexagons become regular hexagons of side length  $(5t - 1)/2 + \sqrt{3}$ , and then scale each obstacle hexagon independently from its center to a hexagon of side length  $(5t - 1)/2$  (see Figure 1.3).



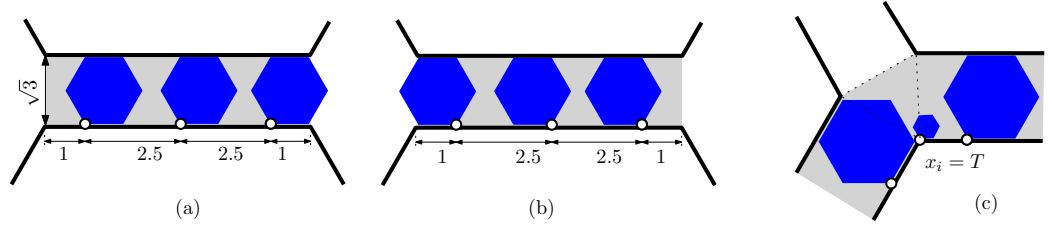


Figure 1.6: (a) A corridor when all unit hexagons are in state R. (b) A corridor where all unit hexagons are in state L. (c) A junction where a small hexagon between two corridors ensures that at most one unit hexagon enters the junction from those corridors.

Between two adjacent obstacle hexagons, there is a  $\frac{5t-1}{2} \times \sqrt{3}$  rectangular corridor. Three adjacent corridors meet at a regular triangle, which we call a junction. For each corridor, there are two junctions adjacent to it; of these two junctions, we denote the junction from which a flag in the corridor enters into as the *active junction* (see Figure 1.7).

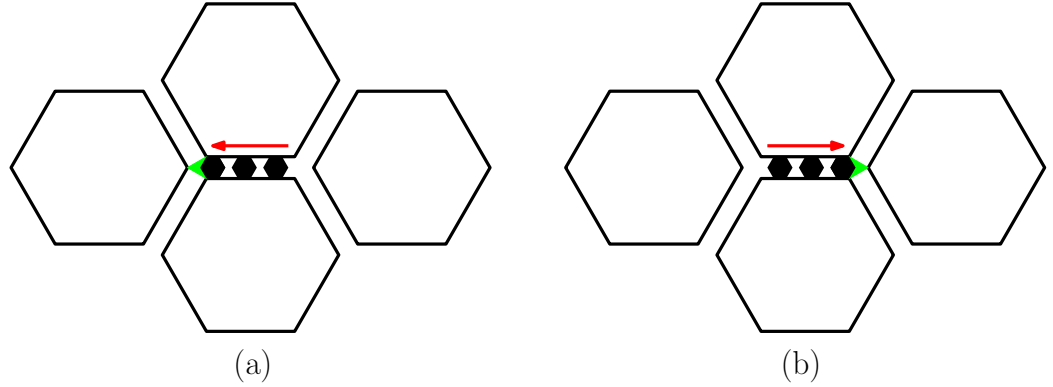


Figure 1.7: The active junction in (a) is the junction on the left and in (b) the active junction is on the right. The active junction is the junction in which a flag enters from a corridor.

We next describe variable, clause, and transmitter gadgets. The basic building block of both variable and transmitter gadgets consists of  $t$  regular hexagons of side length 1 (*unit hexagons*, for short) attached to a wall of a corridor such that the hinges divide the wall into  $t + 1$  intervals of length  $(1, 2.5, \dots, 2.5, 1)$  as shown in Fig. 1.6(a-b) for  $t = 3$ .

In some of the junctions, we attach a small hexagon of side length  $\frac{1}{3}$  to one or two corners of the junction (see Fig. 1.6(c) and Fig. 1.11).

**Variable Gadget.** The **variable gadget** for variable  $x_i$  is constructed as follows. Recall that variable  $x_i$  corresponds to a cycle in the associated graph  $\tilde{A}(\Phi)$ , which has been embedded as a cycle in the hexagonal tiling, with corridors and junctions. In each junction along this cycle, attach a small hexagon in the common boundary of the two corridors in the cycle. Figure 1.8 depicts a *variable gadget* in the hexagonal grid.

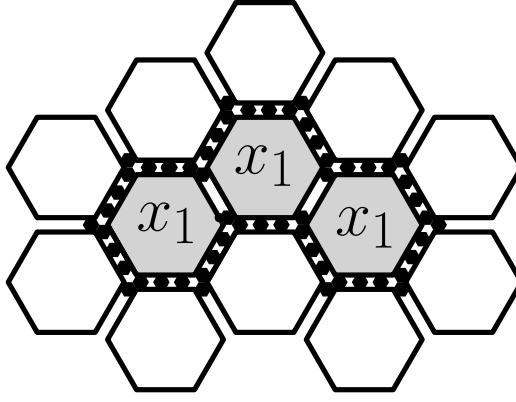


Figure 1.8: This depicts a variable gadget with  $x_1 = T$ . Carefully note that the flags around  $x_1$  are in the state  $R$ . Corridors adjacent to two obstacles of a variable in the honeycomb do not have  $t$  flags; these corridors simply have the flexible hexagons at the junctions.

**Clause Gadget.** Recall that a clause from a Boolean formula  $\Phi$  in 3-CNF has three literals. If  $\Phi$  is a 'yes' instance, then at least one literal in every clause of  $\Phi$  is true. We construct the clause gadget to model this fact about Boolean formulas in 3-CNF.

The **clause gadget** lies at a junction adjacent to three transmitter gadgets (see Fig. 1.9 and Section 1.1). At such a junction, we attach a unit line segment to an arbitrary vertex of the junction, and a small hexagon of side length  $\frac{1}{3}$  to the other end of the segment. If unit hexagons enter the junction from all three corridors (i.e., all three literals are false), then there is no space left for the small hexagon.

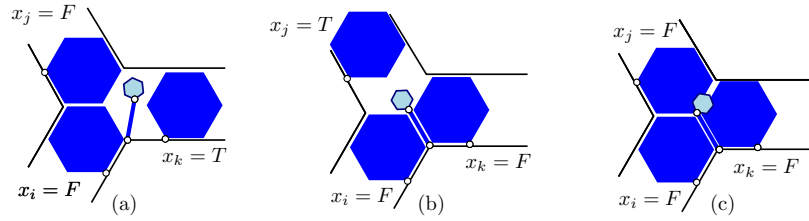


Figure 1.9: (a-b) A clause gadget  $(x_i \vee x_j \vee x_k)$  is realizable when at least one of the literals is TRUE. (c) The clause gadget cannot be realized when all three literals are FALSE.

But if at most two unit hexagons enter the junction (i.e., one of the literals is true), then the unit segment and the small hexagon are realizable.

**Transmitter Gadget.** In the planar 3-SAT graph  $A(\Phi)$ , every variable vertex has an associated cyclic order of edges. Suppose we have a variable vertex  $x_i$  with counter-clockwise cyclic order of edges  $(\{x_i, C_1\}, \{x_i, C_2\}, \dots, \{x_i, C_k\})$ . Assign distinct junctions of the variable cycle of  $x_i$  to the edges  $\{x_i, C_j\}$  in the same cyclic order (refer to Figure ?? for an example).

A **transmitter gadget** is constructed for each edge  $\{x_i, C_j\}$  of the graph  $A(\Phi)$ ; it consists of a sequence of junctions and corridors from a variable gadget's junction to a clause junction.

For each junction in the transmitter gadget, we attach a small hexagon in the junction as shown in Figure 1.11 except at the clause junction. Choosing the location of the small hexagon depends on whether the non-negated or negated literal is found in the clause.

- (a) For an edge  $(x_i, C_j)$  of the graph  $A(\Phi)$ , if the non-negated literal of  $x_i$  exists in  $C_j$ , attach the small

hexagon to the left side of the junction (see Figure 1.10(a)).

- (b) For an edge  $(x_i, C_j)$  of the graph  $A(\Phi)$ , if the negated literal of  $x_i$  exists in  $C_j$ , attach the small hexagon to the right side of the junction (see Figure 1.10(b)).

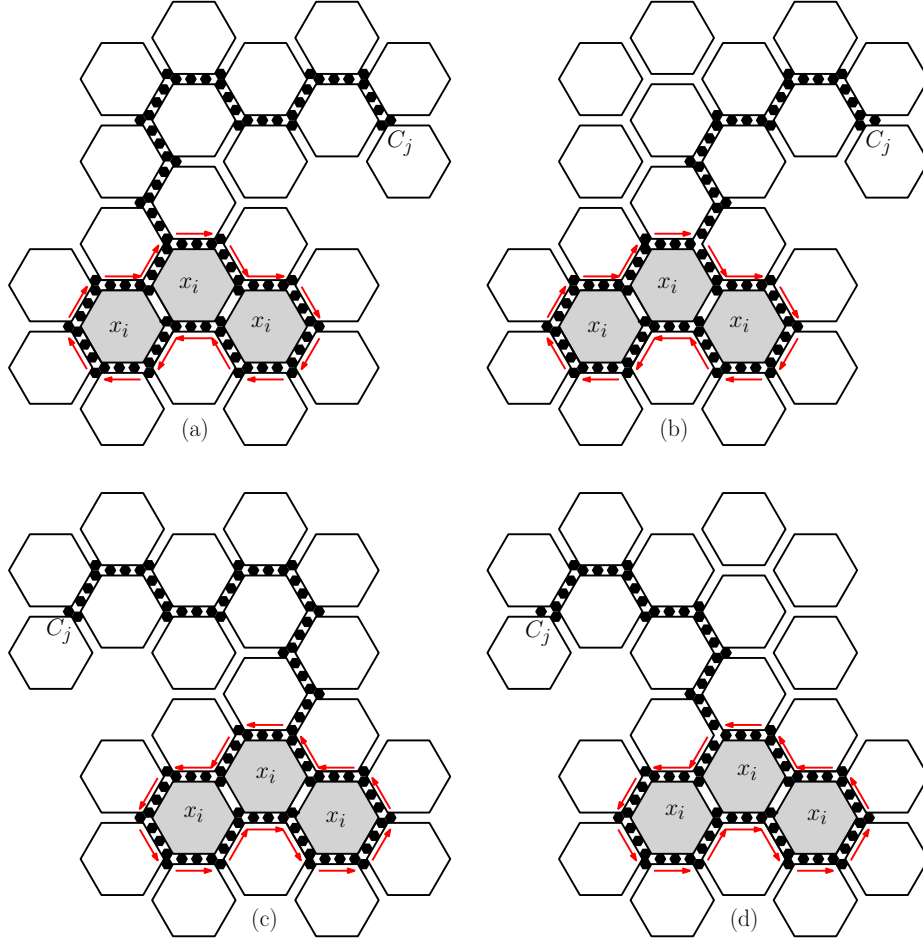


Figure 1.10: These four figures depict an example of placing a transmitter gadget corresponding to edge  $\{x_i, C_j\}$ .

Figure 1.10 shows an example of each rule on choosing a junction to attach a transmitter gadget. The first column transmits a “true” value between the variable gadget and clause junction. The second column transmits a “false” value between the variable gadget and clause junction. The variable gadgets in the first row are in state  $R$ , i.e. variable  $x_i = T$ . The variable gadgets in the second row are in state  $L$ , i.e. variable  $x_i = F$ .

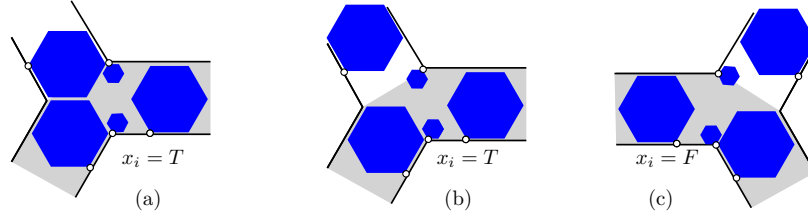


Figure 1.11: The common junction of a variable gadget and a transmitter gadget. (a) When  $x_i = T$ , a hexagon of the transmitter may enter the junction of the variable gadget. (b) When  $x_i = T$ , the transmitter gadget has several possible realizations. (c) When  $x_i = F$ , no hexagon from the transmitter enters a junction of the variable gadget.

### 1.1.1 Functionality of the Auxiliary Construction and Gadgets

If the literal  $x_i$  (resp.,  $\bar{x}_i$ ) appears in  $C_j$ , then we attach a small hexagon to the corner of this junction such that if  $x_i = F$  (resp.,  $\bar{x}_i = F$ ), then the unit hexagon of the transmitter gadget cannot enter this junction.

A variable gadget for vertex  $v$  in the associated graph of a P3SAT Boolean formula encompasses at least  $2 \cdot \deg(v)$  consecutive obstacle hexagons. The arrangement of the consecutive obstacle hexagons are in staggered fashion about a horizontal line where there are at least  $\deg(v)$  obstacle hexagons in the upper portion of the staggering arrangement and at least  $\deg(v)$  obstacle hexagons in the lower portion of the staggering arrangement.

Section 1.1 is a formal description of the auxiliary construction and its gadgets. This subsection covers the underlying assumptions and proofs about the functionality of the auxiliary construction. The first observations about the functionality of the auxiliary construction are about the flags.

*Observation 1.* (1) If the leftmost hexagon is in state R, then all  $t$  hexagons are in state R, and the rightmost hexagon enters the junction on the right of the corridor.

(2) Similarly, if the rightmost hexagon is in state L, then all  $t$  hexagons are in state L, and the leftmost hexagon enters the junction on the left of the corridor.

Observation 1 and the small hexagons ensure that the state of any unit hexagon along the cycle determines the state of all other unit hexagons in the cycle. This property defines the binary variable  $x_i$ : If  $x_i = T$ , then all unit hexagons in the top horizontal corridors are in state R; and if  $x_i = F$ , they are all in state L.

When a binary variable  $x_i = T$ , we will say that the variable is in state *R* and that the cycle of small hexagons around the variable gadget are in a “clockwise direction”. When a binary variable  $x_i = F$ , we will say that the variable is in state *L* and that the cycle of small hexagons around the variable gadget are in a “counter-clockwise direction”.

The proof of the Observation 1 is similar to the proof of Lemma ?? regarding a row in a logic engine having a collision-free configuration.

*Proof.* Suppose the leftmost hexagon,  $h_1$ , is in state *R* in a corridor. Denote the  $t$  flags in a corridor as  $h_1, h_2, \dots, h_t$  from leftmost to rightmost respectively.  $h_2$  must be in state *R* otherwise we result in a collision between  $h_1$  and  $h_2$ . Without loss of generality,  $h_i$  and  $h_{i+1}$  must be in a state *R* in order to prevent an adjacent flag collision. This implies that rightmost flag  $h_t$  must also be in state *R*; this implies that  $h_t$  enters the junction that is on the right of the corridor.

Similarly, suppose the rightmost hexagon,  $h_t$ , is in state *L* in a corridor. Denote the  $t$  flags in a corridor as  $h_1, h_2, \dots, h_t$  from leftmost to rightmost respectively.  $h_{t-1}$  must be in state *L* otherwise we result in a collision between  $h_t$  and  $h_{t-1}$ . Without loss of generality,  $h_i$  and  $h_{i+1}$  must be in a state *L* in order to prevent an adjacent flag collision. This implies that rightmost flag  $h_1$  must also be in state *L*; this implies that  $h_1$  enters the junction that is on the left of the corridor.  $\square$

The flags of the auxiliary construction help communicate the boolean value of a variable gadget to the rest of the auxiliary construction. This communication property of the flags in a corridor is analogous to the flags in a row of a logic engine.

Each junction is a regular triangle, adjacent to three corridors. In some of the junctions, we attach a small hexagon of side length  $\frac{1}{3}$  to one or two corners of the junction (see Fig. 1.6(c) and Fig. 1.11). Importantly, we have the following observation:

*Observation 2.* If a small hexagon is attached to a vertex at a junction between two adjacent corridors, then a flag can enter the junction from at most one of those corridors.

*Proof.* Suppose there is a small hexagon attached to a vertex at a junction between two adjacent corridors. Suppose it is not that case that a flag can enter the junction from at most one of these adjacent corridors. Then there are two flags entering the junction, one from each adjacent corridor. The angular sum of the vertex about the adjacent corridors consists of the obstacle hexagon, both flags, and the small unit hexagon. Each angle of each hexagon is  $\frac{2\pi}{3}$  radians, totalling to an angular sum of  $\frac{8\pi}{3} > 2\pi$ . This is a contradiction with the total angular sum of a vertex on the plane to be  $2\pi$ .  $\square$

Observation 1 and the small hexagons ensure that the state of any unit hexagon along the cycle determines the state of all other unit hexagons in the cycle. This property defines the binary variable  $x_i$ : If  $x_i = T$ , then all unit hexagons in the top horizontal corridors are in state R; and if  $x_i = F$ , they are all in state L.

Suppose there is an edge  $\{x_i, C_j\}$  in the graph  $A(\Phi)$ .

**Lemma 1.** *If  $x_i = T$  and its negated literal is in  $C_j$ , then a flag enters into the clause gadget of  $C_j$ , otherwise it need not enter; if  $x_i = F$  and its non-negated literal is in  $C_j$ , then a flexible hexagon enters into the clause gadget of  $C_j$ , otherwise it need not enter.*

*Proof.* The transmitter gadget for each literal is placed on an active junction of the variable gadget. This junction is “activated” by the variable gadget. By Observation 2, the flag nearest of the transmitter gadget to the variable gadget does not enter the transmitter-variable junction. By Observation 1 and the state of the flag nearest of the transmitter gadget to the variable gadget implies that the flags in that transmitter corridor activate the junction opposite the transmitter-variable junction. The subsequent flags in the transmitter gadget corridors have the same state of the flag in the transmitter gadget nearest of the transmitter-variable junction by Observations 1 and 2. This activation process continues up to the clause junction and the flag in the transmitter gadget nearest the clause junction enters the clause junction.  $\square$

**Lemma 2.** *Hexagons in a clause junction have a non-overlapping placement if and only if at least one of the three literals is true.*

*Proof.* Suppose we have a hexagons in a clause junction that have a non-overlapping placement. To show that there is at least one of the three literals is true, we do a proof by contradiction. Suppose all literals of the clause are false. If all literals of the clause are false, then all flags in each transmitter gadget nearest their clause junction enters the clause junction, as shown in Figure 1.9(c) which show the small hexagon overlapping flags in the clause junction, a contradiction with hexagons in the clause junction have a non-overlapping placement.

If at least one of the three literals is true, then by Lemma 1, this literal’s flag need not enter the transmitter-variable junction. There allows for the small hexagon in the clause junction to move into the area where this literal’s flag could enter the junction and thus allow non-overlapping placement of hexagons in the junction.  $\square$

For a variable gadget  $x_i$ , place horizontal axis  $h$  at mid-height of the gadget. Then we have the following lemma:

**Lemma 3.** *If variable  $x_i = T$ , then all flags above  $h$  are in state  $R$  and all flags below  $h$  are in state  $L$ ; if variable  $x_i = L$ , then all flexible hexagons above  $h$  are in state  $L$  and all flexible hexagons below  $h$  are in state  $R$ .*

*Proof.* Suppose we have two adjacent corridors  $k_i$  and  $k_{i+1}$  sharing junction  $J_i$  and without loss of generality,  $k_i$  is the left most corridor. Observation 2 implies that there can only be one hexagon entering  $J_i$  from either  $k_i$  or  $k_{i+1}$ . If the hexagon that enters  $J_i$  is from corridor  $k_i$ , then this hexagon has state  $R$  and all flags in corridor  $k_i$  are in state  $R$  by Observation 1. Since the nearest flag of corridor  $k_{i+1}$  cannot enter the junction  $J_i$ , it must also have state  $R$ . All flags in corridor  $k_{i+1}$  are in state  $R$  by Observation 1.

The argument is similar if the hexagon entering  $J_i$  is from corridor  $k_{i+1}$  and all flags in both corridors  $k_i$  and  $k_{i+1}$  have state  $L$ .

Because variable gadgets form a simple cycle of corridors and junctions  $(k_1, J_1, k_2, J_2, \dots, k_n, J_n)$  and the argument above, all flags about a variable gadget have the same state.  $\square$

**Lemma 4.** *For every instance  $\Phi$  of P3SAT, the above polygonal linkage with flexible and obstacle polygons has the following properties: (1) it has polynomial size; (2) its hinge graph is a forest; (3) it admits a realization such that the obstacle polygons remain fixed if and only if  $\Phi$  is satisfiable.*

*Proof.* (1) We can bound the number of obstacle hexagons to represent a variable gadget by  $2D$ , where  $D = (\max_{v \in V} \deg(v))$ . The number of clause junctions is  $n$ . To give an upper bound on the number of flags in the auxiliary construction, we have to account for the flags in the transmitter gadgets, the extra hexagons found in junctions, and the flexible hexagons around the variable gadgets.

Recall that the number of flags in a corridor are  $t = 2N(m, n)^3 + 1$  where  $N(m, n)$  is a polynomial. Recall that the drawing of  $A(\Phi)$  have edges drawn in vertically and horizontally and can join at some “elbow”. The distance can be measured in the  $\ell_1$  norm. Similarly in the honeycomb construction, the flexible hexagons zig-zig vertically and horizontally through out honeycomb. The number of corridors about an obstacle hexagon is 6. To give a generous upper bound on the number of flags in a transmitter gadget, is  $6 \cdot t \cdot \ell_1(v_i, C_j)$ , assuming each obstacle hexagon is of unit height.

The number of junctions in the auxiliary construction is the number of junctions to form all variable gadgets, transmitter gadgets, and clause gadgets. We know there are at most  $2 \cdot D$  obstacle hexagons to form each variable gadget and 6 junctions for each obstacle hexagon. Therefore an upper bound for the number of flags around variable gadgets is  $m \cdot 6 \cdot t \cdot 2 \cdot D$ . The upper bound for the number of junctions in a transmitter gadget is  $6\ell_1(v_i, C_j)$ . Thus, the upper bound of all junctions in all transmitter gadgets is

$$6 \cdot \sum_{\{v_i, C_j\} \in E} \ell_1(v_i, C_j).$$

The upper bound on the total number of flags is

$$m \cdot 6 \cdot t \cdot 2 \cdot D + 6 \cdot \sum_{\{v_i, C_j\} \in E} \ell_1(v_i, C_j).$$

(2) Recall that a forest is a disjoint union of trees. By construction, each flag is hinged to exactly one obstacle hexagon. There are no hinges between obstacle hexagons. Consequently, each component of the hinge graph is a star, where the center corresponds to an obstacle hexagon and the leafs corresponds to the flexible hexagons attached to it.

(3) The final statement is to show an if and only if statement: it admits a realization such that the obstacle polygons remain fixed if and only if  $\Phi$  is satisfiable.

Suppose  $\Phi$  is satisfiable. Each variable has a boolean value and we can encode the corresponding auxiliary construction accordingly. For each variable, we encode the boolean value by the state of the flags surrounding the variable gadget to  $R$  or  $L$ . Lemma 3 shows that the corridors and junctions around the variable gadget are realizable. Lemma 1 also show that for each transmitter gadget, every corridor and junction are also realizable. Lemma 2 shows that there is at least one hexagon in the clause junction and that the clause is realizable. Thus all parts of the auxiliary construction realizable and thus we have a realization.

Suppose the construction admits a realization such that the obstacle polygons remain fixed. Each variable gadget's flags are configured to state  $L$  or  $R$ . The variable's corresponding state correspond to the variable's truth value, i.e.  $R$  for true and  $L$  for false. Using Lemma 3, the boolean state of the variable gadget is transmitted to all transmitter gadgets associated to it. Each clause is realizable and so for every clause, there exists one true literal in the clause corresponding to a variable by Lemma 2. If every clause has some true literal, then the corresponding 3-CNF boolean formula is satisfiable.  $\square$

**Modified Auxiliary Construction.** Recall that in Theorem 1 we want to show that it is strongly NP-hard to decide whether a polygonal linkage whose hinge graph is a tree can be realized with counter-clockwise orientation. We modify the auxiliary construction allowing all polygons to move freely, and by adding extra polygons and hinges so that the hinge graph becomes a *tree*, and the size of the construction remains polynomial. The auxiliary construction is based on a polynomial sized area of the hexagonal grid, using obstacle hexagons of side lengths  $N(n, m)$ , unit hexagons (of side length 1), and small hexagons of side length  $\frac{1}{3}$ . We modify it in five steps as follows:

1. Move the obstacle hexagons apart such that the width of each corridor increases from  $\sqrt{3}$  to  $\sqrt{3} + 1/(100N)$ .
2. Replace the unit segment in each clause gadget by a skinny rhombus of diameter  $\sqrt{1 + (100N)^{-2}}$  and width  $1/(100N)$ .
3. Enclose the regular hexagon region  $J$  containing all gadgets by a *frame* of 6 congruent regular hexagons, as shown in Fig. 1.14(a), hinged together in a path.
4. Connect the frame and the obstacles in  $J$  into a simply connected polygonal linkage: in each obstacle hexagon, the bottom side is adjacent to the frame or to a corridor. Introduce a hinge at the midpoint of one such side in each obstacle hexagon. If this side is adjacent to the frame, then attach the hinge to the frame. Otherwise, the hinge is attached to a new *connector* polygon: a skinny rhombus of diameter 1 and width  $\frac{1}{100N}$ . The far corner of each rhombus is hinged to the unit hexagon in the middle of the corridor at shown in Figure 1.14(b).
5. The construction so far constains rows and columns of obstacle hexagons. Every other column of obstacle hexagons is hinged to the bottom side of the perimeter of  $J$ .

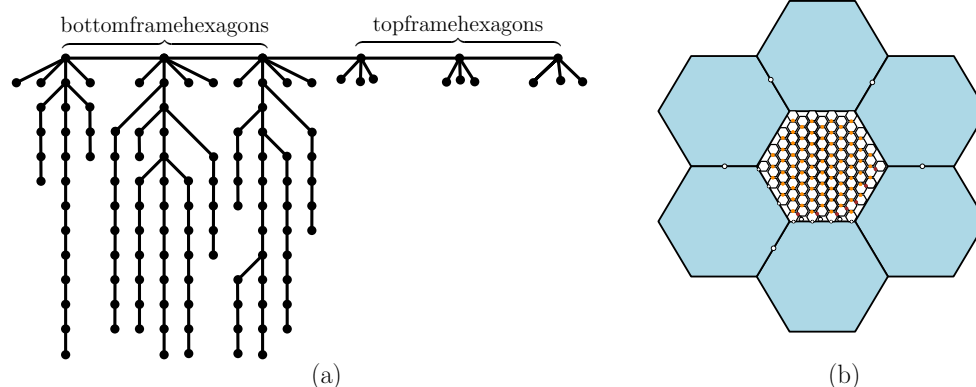


Figure 1.12: (a) illustrates a tree corresponding to the modified auxiliary construction in (b). On the left half of the tree, we have the bottom most frame hexagons and the hexagons in the interior of  $J$  as children of the bottom frame hexagons. The top most frame hexagons only have the half sized hexagons attached to them. (b) is the corresponding modified auxiliary construction.

These bottom most obstacle hexagons have a hinge point on its side. The columns that do not have an obstacle hexagon hinged to the perimeter of  $J$  has a half-sized hexagon hinged to the perimeter of  $J$  and a locked flag with no state to the first obstacle hexagon above it (See Figure 1.13).

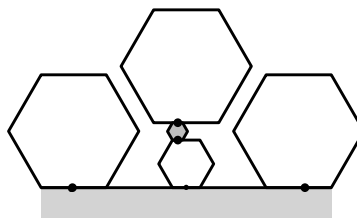


Figure 1.13: In this figure we illustrate the bottom of the perimeter of  $J$  with three obstacle hexagons, a half sized hexagon, and a locked flag whose hinge points lock the flag's state (becoming stateless).

We obtain a simply connected polygonal linkage. We now allow the obstacle hexagons to move freely, and call their original fixed position *canonical*. (3) We may assume without loss of generality that the frame is at its original position. It is enough to show that the obstacle hexagons are still confined to an  $1/N$ -neighborhood of their canonical position, then it follows that the polygonal linkage is realizable if and only if  $\Phi$  is satisfiable.





Figure 1.14: (a) A frame (built of 6 hinged regular hexagons) encloses a hexagonal tiling, and vertical paths connect all obstacle hexagons to the frame. (b) A corridor is widened to  $\sqrt{3} + \frac{1}{100N}$ . A connection between two adjacent obstacle hexagons is established via a skinny rhombus.

The position of each hexagon can be defined by the isometry from its canonical position; an isometry is given by the triple  $(\alpha, \beta, \delta)$  where  $\alpha$  is a counter clockwise rotation about the center of the hexagon and  $(\beta, \delta)$  is a translation vector. Canonical position would have each obstacle hexagon's position as  $(0, 0, 0)$ .

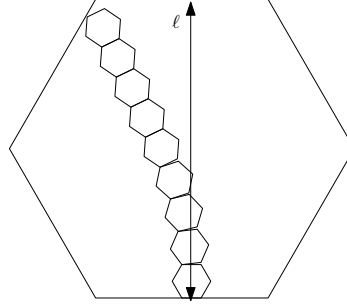


Figure 1.15: This figure depicts a column of obstacle hexagons rotated such that the obstacle hexagons veer of the vertical line  $\ell$ .

**Lemma 5.** *Let  $P$  be a polygonal linkage obtained from the modified auxiliary construction. In every realization of  $P$ , the obstacle polygons are close to canonical position such that*

Lemma 5 serves as assurance that once a boolean formula of P3SAT is encoded into an arbitrary realization of the modified auxiliary construction, the information of the boolean formula is preserved regardless of the positioning of the gadgets and components in the construction. This quality shows that the information is stable and preserved in an arbitrary realization of the modified auxiliary construction. In Figure 1.15, we have a column of obstacle hexagons veering off  $\ell$ . This is an example of extreme angular rotation that should not occur over a vertical stack of hexagons.

*Proof.* We need to show that the modified auxiliary construction could not deform in such a way that any information the construction encodes is lost or modified and the functionality of the gadgets within the construction behave as stated in the description.

To help identify components of the construction for this proof, let's identify components in the canonical position:



Figure 1.16: (a) depicts a column of obstacle hexagons  $O_1, \dots, O_{10}$  along the vertical line  $\ell$ ; (b) identifies obstacle hexagons  $O_1, \dots, O_{10}$  in (a).

Without loss of generality, we can identify a column of obstacle hexagons  $O_i$  along a vertical line  $\ell$  (See Figure 1.16). In this proof, unless otherwise specified, we assume that the argument refers to a column that starts and ends with an obstacle hexagon. In total there will be  $u + 1$  number of obstacle hexagons and  $u$  corridors in a column. Note that:

$$\begin{aligned}
 u &= \frac{J_h(z)}{2} - \frac{1}{2} \\
 &= \frac{1}{2} (6z + 1 - 1) \\
 &= 3z \\
 &= 12s
 \end{aligned}$$

where  $J_h$  is defined in Equation 1.1.

The length of  $H(n, m)$  (and  $\ell$  in Figure 1.17(a)) can be expressed as a sum of the heights of the corridors and obstacle polygons. The width of a skinny rhombus in canonical position is  $\frac{1}{100N}$ . The obstacle hexagon has height of  $2s(n, m) \cdot \sqrt{3}$ , and the flag is of height  $\sqrt{3}$ .

$$H(n, m) = (12s(n, m) + 1) 2s(n, m) \sqrt{3} + 12s(n, m) \left( \frac{1}{100N} + \sqrt{3} \right) \quad (1.4)$$

The cross section of the corridor must have a minimum height of  $\sqrt{3}$  everywhere. The height of the  $i^{\text{th}}$  obstacle polygon in noncanonical position is  $2s(n, m) \sec(\alpha_i) \cdot \sqrt{3}$  (see Figure 1.18 for reference).

**Angular Rotation  $\alpha$ .** First we show that the angular rotation of the obstacle hexagons with respect to canonical position is small. We first look at the relative angular difference between two adjacent obstacle polygons

$$|\alpha_i - \alpha_{i+1}|.$$

Given an arbitrary instance of a modified auxiliary construction, consider  $O_i$ ,  $O_{i+1}$ , and the corridor between  $O_i$  and  $O_{i+1}$ . The skinny rhombus has length  $\sqrt{1 + (100N)^{-2}}$ .

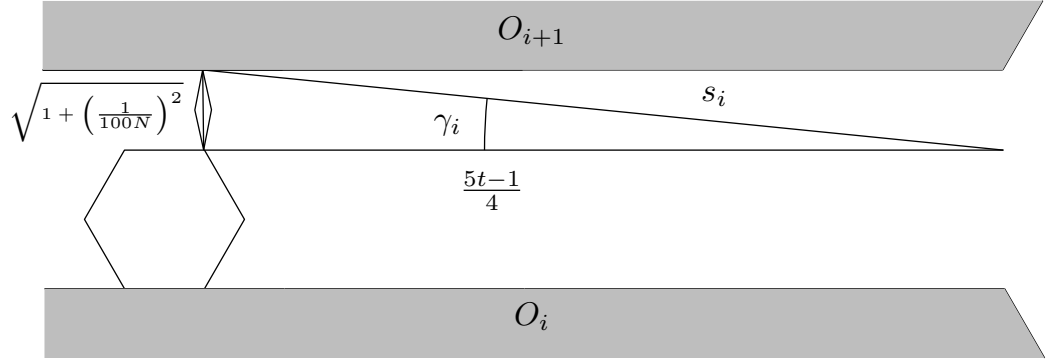


Figure 1.17: The obstacle hexagon here is in noncanonical position, and showing the side lengths adjacent to  $\alpha_i$ .

In Figure 1.16(a) we see  $\ell$  in the center of the column of obstacle hexagons. Our goal is to show that the column of hexagons cannot tilt in the manner shown in Figure 1.15 where the column veers greatly into the space occupied by other corridors and obstacle hexagons. The cross section of an arbitrary corridor must have a height of at least  $\sqrt{3}$  everywhere. Otherwise, a flag would overlap with an obstacle hexagon; it would no longer remain a realization since the height of a flag is  $\sqrt{3}$ . In Figure 1.17, we illustrate an obstacle hexagon, its upper corridor with the flag that has the hinge to the skinny rhombus. The rhombus is hinged at the midpoint of the upper side of the corridor. The length from a corridor's midpoint to one end of the corridor is  $\frac{5t-1}{4}$ .  $\gamma_i$  is the angle between  $\zeta_i$  and the horizontal axis at the height of the flag ( $i = 1, 2, \dots, u$ ). The bound of  $\gamma_i$  is:

$$\begin{aligned}
 \gamma_i &\leq \tan^{-1} \left( \frac{\sqrt{1 + (\frac{1}{100N})^2}}{\frac{5t-1}{4}} \right) \\
 &= \tan^{-1} \left( \frac{4 \cdot \sqrt{1 + (\frac{1}{100N})^2}}{5t-1} \right) \\
 &\leq \frac{4 \cdot \sqrt{1 + \frac{1}{(100N)^2}}}{5t-1} \\
 &\leq \frac{\sqrt{16 + \frac{16}{(100N)^2}}}{10N^3-6} \\
 &\leq \frac{5}{10N^3-6} \\
 &\leq \frac{5}{10N^3-10} \\
 &\leq \frac{1}{2(N^3-1)}
 \end{aligned} \tag{1.5}$$

Inequality 1.5 uses the first two terms Maclaurin series of  $\tan^{-1}$ . Thus the relative rotational difference between adjacent obstacle hexagons is

$$|\alpha_i - \alpha_{i+1}| \leq \frac{1}{2(N^3-1)} \tag{1.6}$$

The relative difference between  $\alpha_i$  and  $\alpha_{i+1}$  is small. From Figure 1.13, we know that the bottom most obstacle hexagon is hinged to the frame. This implies that  $\alpha_1 = 0$  and

$$|\alpha_1 - \alpha_2| = |\alpha_2| \leq \frac{1}{2(N^3-1)}.$$

There are a total of  $u$  obstacle hexagons in a column with possibly up to  $u-1$  nonzero obstacle hexagons

rotations. We can derive 1) a bounded sum of rotational displacement over a column of obstacle hexagons:

$$\sum_{i=1}^{u-1} |\alpha_i - \alpha_{i+1}| \leq \frac{u-1}{2(N^3-1)} \quad (1.7)$$

and 2) derive the maximum rotational displacement at the  $i^{\text{th}}$  obstacle hexagon:

$$\alpha_i \leq \sum_{j=1}^i \frac{j}{2(N^3-1)} = \frac{(i^2+i)}{4(N^3-1)} \quad (1.8)$$

The sum of total displacement in a given column is bounded by:

$$|\alpha_u| \leq \sum_{i=2}^{u-1} |\alpha_i - \alpha_{i+1}| \leq \frac{u-1}{2(N^3-1)} = \frac{12s-1}{2((c_Ns)^3-1)}$$

**Vertical Displacement  $\delta$**  When an obstacle hexagon is rotated by  $\alpha_i$ , the height of the hexagon becomes  $2s(n,m)\sqrt{3}\sec\alpha_i$ . Figure 1.18 shows the geometry of a rotated obstacle hexagon.

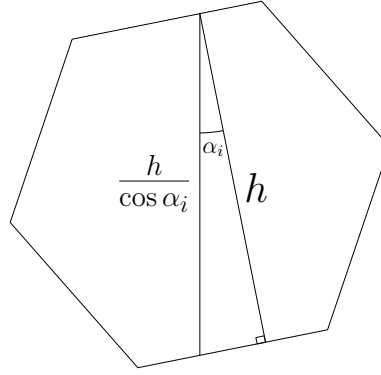


Figure 1.18: This figure shows a right triangle with angle  $\alpha_i$  and sides of length  $h$  and  $\frac{h}{\cos\alpha_i}$ .

To show that the vertical displacement from canonical position is small, we first consider a column of obstacle hexagons in canonical position (see Figure 1.19). For canonical position, the  $j^{\text{th}}$  obstacle has  $\delta_j = 0$ .

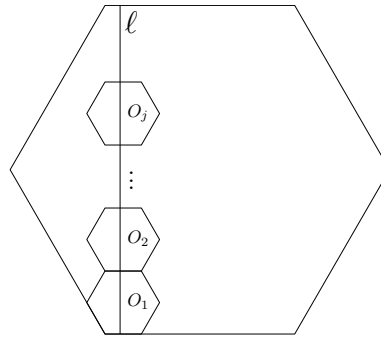


Figure 1.19: This illustration is of a column of obstacle hexagons in canonical position along a vertical line segment  $\ell$ .

From Equation 1.4, we know the exact height of  $\ell$  in terms of the heights of the corridors and obstacle hexagons in canonical position. Consider the first  $j$  terms for the height of the column of obstacle hexagons and corridors for an arbitrary construction with angular rotation and vertical displacement for *one* obstacle

hexagon  $|\delta_v| > 0$ , where  $j = 2, \dots, u+1$  and  $1 < v \leq j$ .

$$\begin{aligned}
\sum_{i=1}^j \left( 2\sqrt{3}s \sec(\alpha_i) \right) + \delta_v + (j-1) \left( \frac{1}{100N} + \sqrt{3} \right) &\leq j \cdot 2s\sqrt{3} + (j-1) \cdot \left( \frac{1}{100N} + \sqrt{3} \right) \\
2\sqrt{3}s \sum_{i=1}^j \sec(\alpha_i) + \delta_v &\leq j \cdot 2s\sqrt{3} \\
\sum_{i=1}^j \sec(\alpha_i) + \delta_v &\leq j \\
\delta_v &\leq j - \sum_{i=1}^j \sec(\alpha_i) \\
\delta_v &\leq j - \left( j - \sum_{i=1}^j \frac{\alpha_i^2}{2} \right) \\
\delta_v &\leq \sum_{i=1}^j \frac{\alpha_i^2}{2}
\end{aligned}$$

Using Inequalities 1.7 and 1.8, we derive the following result:

$$\begin{aligned}
\sum_{i=1}^j \frac{\alpha_i^2}{2} &\leq \frac{\sum_{i=1}^j \left( \sum_{\kappa=1}^i \frac{\kappa}{2(N^3-1)} \right)^2}{2} \\
\sum_{i=1}^j \alpha_i^2 &\leq \sum_{i=1}^j \left( \sum_{\kappa=1}^i \frac{\kappa}{2(N^3-1)} \right)^2 \\
&\leq \sum_{i=1}^j \left( \frac{1}{2(N^3-1)} \sum_{\kappa=1}^i \kappa \right)^2 \\
&\leq \sum_{i=1}^j \left( \frac{1}{2(N^3-1)} \cdot \frac{i^2+i}{2} \right)^2 \\
&\leq \sum_{i=1}^j \left( \frac{i^2+i}{4(N^3-1)} \right)^2
\end{aligned}$$

Thus we finally say that the bound for  $\delta_v$ , where  $1 < v \leq j$ , is small:

$$\delta_v \leq \frac{\sum_{i=1}^j \left( \frac{i^2+i}{4(N^3-1)} \right)^2}{2} \tag{1.9}$$

**Horizontal Displacement  $\beta$**  We show the horizontal displacement of an obstacle hexagon is small. First we analyze the change of corridor's cross-section with respect to horizontal displacement.

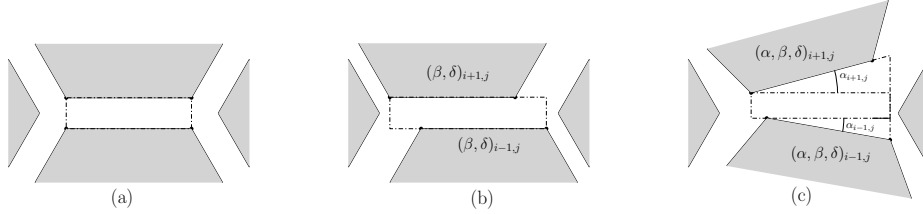


Figure 1.20: (a) A corridor and corresponding junctions in canonical position with cross section  $N(n, m) \times (\sqrt{3} + (100N)^{-1})$ . (b) A corridor whose total horizontal displacement is  $\beta_{i+1} + \beta_{i-1}$  on the top and total vertical displacement of  $\delta_{i+1} + \delta_{i-1}$  on the bottom; its cross section is  $(N(n, m) + \beta_{i+1} + \beta_{i-1}) \times (\sqrt{3} + (100N)^{-1}) + \delta_{i+1} + \delta_{i-1}$ . (c) shows the cross sectional area of a corridor with full rotational, horizontal, and vertical displacement.

Figure 1.20 shows the same corridor and corresponding junctions in canonical position and non-canonical positions. This figure is of a corridor and adjacent junctions formed by obstacle hexagons in counter-clockwise order:  $O_{i-1,j}$ ,  $O_{i,j-1}$ ,  $O_{i+1,j}$ , and  $O_{i,j+1}$ . The cross sectional areas for Figure 1.20(a) and Figure 1.20(b) are  $N(n, m) \times (\sqrt{3} + (100N)^{-1})$  and  $(N(n, m) + \beta_{i+1} + \beta_{i-1}) \times (\sqrt{3} + (100N)^{-1}) + \delta_{i+1} + \delta_{i-1}$  respectively. Figure 1.20(c) shows the same corridor with rotational, horizontal, and vertical displacement. To find the cross sectional area of the corridor in Figure 1.20(c), we decompose it into three parts, the upper triangle, the rectangle, and the lower triangle.

We're given  $N(n, m)$  and  $(\alpha, \beta, \delta)_{i,j}$  for all  $i, j = 1, \dots, u$ . The area of the upper triangle is

$$\frac{1}{2} (N + \beta_{i+1} + \beta_{i-1})^2 \tan(\alpha_{i+1,j}). \quad (1.10)$$

The area of the rectangle is

$$(N + \beta_{i+1} + \beta_{i-1}) \cdot \left( (\sqrt{3} + (100N)^{-1}) + \delta_{i+1} + \delta_{i-1} \right). \quad (1.11)$$

The area of the lower triangle is

$$\frac{1}{2} (N \cdot \cos(\alpha_{i-1,j})) \cdot (N \cdot \sin(\alpha_{i-1,j})) = N^2 \sin(2 \cdot \alpha_{i-1,j}). \quad (1.12)$$

We show by an induction argument that the horizontal displacement for any given modified construction is small. Consider a column of obstacle hexagons which has an obstacle hexagon  $O_1$  hinged at the bottom of the frame  $J_z$ . The obstacle hexagon  $O_1$  has no displacement; it is immobile. Consider the case where the column of hexagon has a half sized hexagon attached at the the bottom of the frame, the hinge points of the half sized hexagon immobilize the the first obstacle hexagon of that column (see Figure 1.13 for reference). In either case the obstacle hexagon  $O_2$  has horizontal mobility by way of the range of motion from the skinny rhombi (see Figure 1.23 for reference) between  $O_1$  and  $O_2$ . The diameter of the skinny rhombi are  $\sqrt{1 + (100N)^{-1}}$ ; the possible horizontal displacement  $O_2$  could have is  $\sqrt{1 + (100N)^{-1}}$  plus the horizontal displacement contributed by  $\alpha_{i,2}$  (see Figure ??).

$$\beta_{i,2} \leq \sqrt{1 + (100N)^{-1}} + \frac{h}{2} \sin \alpha_{i,2} \leq \sqrt{1 + (100N)^{-1}} + \frac{h\alpha_{i,2}}{2} \quad (1.13)$$

The maximal horizontal displacement is shown in Inequality 1.13 where  $h$  is the height of an obstacle hexagon. The maximal horizontal displacement is  $\beta_{i,2} = \sqrt{1 + (100N)^{-1}} + \frac{h}{2} \sin \alpha_{i,2}$  however, this large value is infeasible. We will now show what the feasible upper bound of horizontal displacement is. Firstly, the range of motion of the skinny rhombus is limited by the vertical displacement of an obstacle hexagon. Secondly, we have bounded the angular displacement  $\alpha$  of an obstacle hexagon.

The vertical displacement of the  $v^{\text{th}}$  obstacle hexagon is:

$$\delta_v \leq \frac{\sum_{i=1}^v \left( \frac{5(i^2+i)}{20N^3-12} \right)^2}{2}$$

Let the angular rotation of the skinny rhombus be  $\omega_v$ , then corresponding horizontal displacement  $\phi$  is:

$$\phi = \frac{\delta_v}{\tan(\omega_v)} = \frac{\delta_v}{\tan\left(\sin^{-1}\left(\frac{\delta_v}{\sqrt{1+\left(\frac{1}{100N}\right)^2}}\right)\right)}$$

using Maclaurin series,  $\phi$  simplifies to:

$$\begin{aligned} \frac{\delta_v}{\tan\left(\sin^{-1}\left(\frac{\delta_v}{\sqrt{1+\left(\frac{1}{100N}\right)^2}}\right)\right)} &\leq \frac{\delta_v}{\tan\left(\frac{\delta_v}{\sqrt{1+\left(\frac{1}{100N}\right)^2}} + \frac{1}{6}\left(\frac{\delta_v}{\sqrt{1+\left(\frac{1}{100N}\right)^2}}\right)^3\right)} \\ &\leq \frac{\delta_v}{\frac{\delta_v}{\sqrt{1+\left(\frac{1}{100N}\right)^2}} + \frac{1}{6}\left(\frac{\delta_v}{\sqrt{1+\left(\frac{1}{100N}\right)^2}}\right)^3} \end{aligned}$$

The angular displacement of the  $v^{\text{th}}$  obstacle hexagon is:

$$\alpha_v \leq \frac{(v^2 + v) 5}{2(10N^3 - 6)}$$

which implies:

$$\frac{h\alpha_2}{2} \leq \frac{15h}{2(10N^3 - 6)}$$

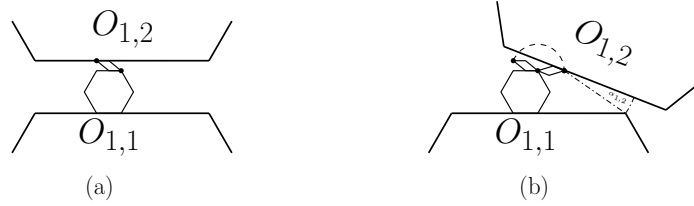


Figure 1.21: This figure illustrates the possible range of motion of the skinny rhombus between two obstacle hexagons and the feasible range of rotational displacement of  $O_{1,2}$ .

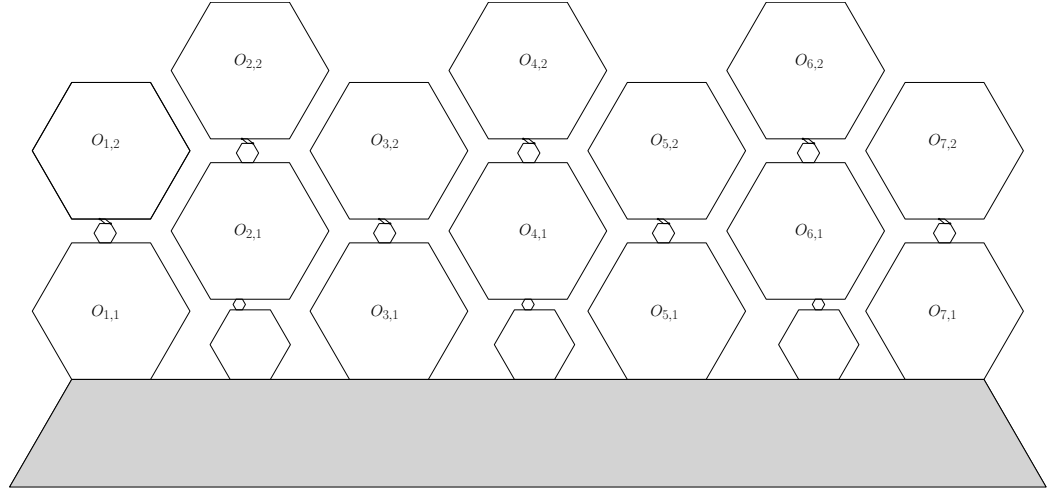


Figure 1.22: bottom

Note that the bottom most obstacle hexagon  $O_{j,1}$  is hinged to the frame or hinged to some half sized hexagon such that  $\beta_{j,1} = 0$ . The range of motion horizontal motion that  $O_{j,2}$  has is dictated by the range of possible motion from the skinny rhombus between  $O_{j,1}$  and  $O_{j,2}$ . The diameter of the skinny rhombus is  $\sqrt{1 + (100N)^{-1}}$ . If  $\beta_{j,2} = \pm\sqrt{1 + (100N)^{-1}}$ , there would be a collision a corridor(s) adjacent to  $O_{j,2}$ .

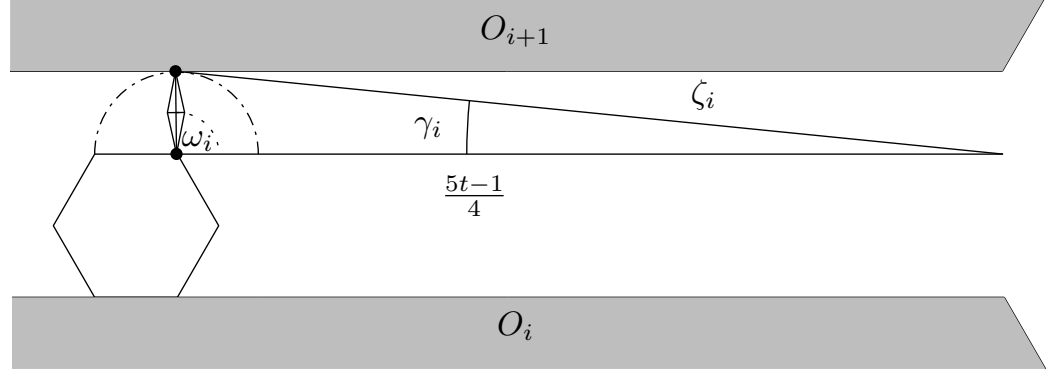


Figure 1.23: The full range of motion is shown dashed half circle about the diameter of the skinny rhombus.

Figure 1.23 shows the range of motion of the skinny rhombus. The angle formed between the diameter of the rhombus and the half length of the corridor is  $\omega_i$ . The relative difference between  $\square$



## Chapter 2

### Realizability Problems for Weighted Trees

#### 2.1 Properties for Weighted Trees and Polygonal Linkages

In order to perform our analysis for weighted trees and polygonal linkages, we'll want to use a suitable metric. The usual Euclidian distance will not suffice for this analysis and so we turn to the Hausdorff distance.

**Hausdorff Distance** Let  $A$  and  $B$  be sets in the plane. The *directed Hausdorff distance* is

$$d(A, B) = \sup_{a \in A} \inf_{b \in B} \|a - b\| \quad (2.1)$$

$h(A, B)$  finds the furthest point  $a \in A$  from any point in  $B$ . *Hausdorff distance* is

$$D(A, B) = \max \{d(A, B), d(B, A)\} \quad (2.2)$$

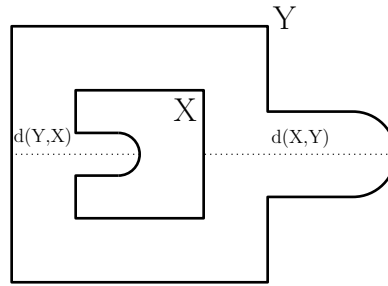


Figure 2.1: An illustrative example of  $d(X, Y)$  and  $d(Y, X)$  where  $X$  is the inner curve, and  $Y$  is the outer curve.

**$\varepsilon$ -approximation** The weighted graph,  $G$ , is an  $\varepsilon$ -approximation of a polygon  $P$  if the Hausdorff distance between every realization such realization of  $G$  as a contact graph of disks and a congruent copy of  $P$  is at most epsilon. A weighted graph  $G$  is said to be a  $O(f(x))$ -approximation of a polygon  $P$  if there is a positive constant  $M$  such that for all sufficiently large values of  $x$  the Hausdorff distance between every realization such realization of  $G$  as a contact graph of disks and a congruent copy of  $P$  is at  $M \cdot |f(x)|$ . A weighted graph  $G$  is said to be a *stable* if it has the property that for every two such realizations of  $G$ , the distance between the centers of the corresponding disks is at most  $\varepsilon$  after a suitable rigid transformation.

#### 2.2 Approximating Regular Hexagons with Snowflakes

In figure 2.2, we have a set of unit radius disks (circles) arranged in a manner that outlines regular, concentric hexagons.

**Problem 1** (Approximating Polygonal Shapes with Contact Graphs). For every  $\varepsilon > 0$  and polygon  $P$ , there exists a contact graph  $G = (V, E)$  such that the Hausdorff distance  $d(P, G) < \varepsilon$

Recall problems (??) and (??): given a positive weighted tree,  $T$ , is  $T$  the (ordered) contact graph of some disk arrangement where the radii are equal to the vertex weights. For now, we'll focus on a particular family

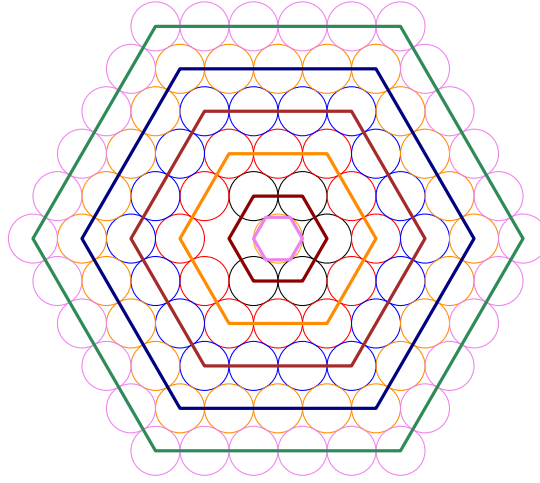


Figure 2.2: A contact graph that resembles the shape of concentric hexagons.

of this problem space where the weighted trees can be realized as a *snowflake*. For  $i \in \mathbb{N}$ , the construction of the snowflake tree,  $S_i$ , is as follows:

- Let  $v_0$  be a vertex that has six paths attached to it:  $p_1, p_2, \dots, p_6$ . Each path has  $i$  vertices.
- For every other path  $p_1, p_3$ , and  $p_5$ :
  - Each vertex on that path has two paths attached, one path on each side of  $p_k$ .
  - The number of vertices that lie on the path attached to the  $j^{\text{th}}$  vertex of  $p_k$  is  $i - j$ .

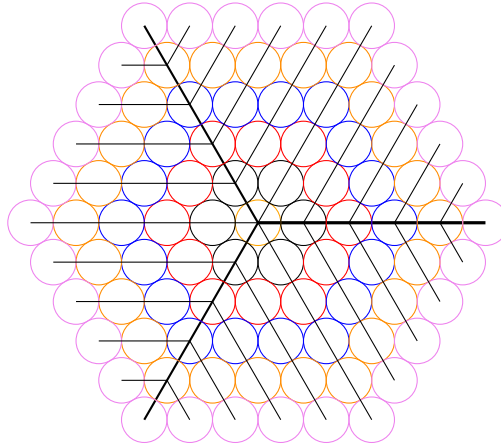


Figure 2.3: The same contact graph as in figure 2.2 overlaid with the a perfectly weighted snowflake tree.

A *perfectly weighted snowflake tree* is a snowflake tree with all vertices having weight  $\frac{1}{2}$ . A *perturbed snowflake tree* is a snowflake tree with all vertices having weight of 1 with the exception of  $v_0$ ; in a perturbed snowflake tree,  $v_0$  will have a weight of  $\frac{1}{2} + \gamma$ . For our analysis, all realizations of any snowflake, perfect or perturbed, shall have  $v_0$  fixed at origin. This is said to be the canonical position under Hausdorff distance of the snowflake tree.

**Perfectly Weighted Snowflake Tree.** Consider the graph of the triangular lattice with unit distant edges:

$$\begin{aligned} V &= \left\{ a \cdot (1,0) + b \cdot \left( \frac{1}{2}, \frac{\sqrt{3}}{2} \right) : a, b \in \mathbb{Z} \right\} \\ E &= \{ \{u, v\} : \|u - v\| = 1 \text{ and } u, v \in V \} \end{aligned}$$

The following graph,  $G = (V, E)$  is said to be the *unit distance graph* of the triangular lattice. We can show that no two distinct edges of this graph are non-crossing. First suppose that there were two distinct edges that crossed,  $\{u_1, v_1\}$  and  $\{u_2, v_2\}$ . With respect to  $u_1$ , there are 6 possible edges corresponding to it, with each edge  $\frac{\pi}{3}$  radians away from the next. Neither edge crosses another; and so we have a contradiction that there are no edge crossings with  $\{u_1, v_1\}$ .

The perfectly weighted snowflake tree that is a subgraph over the *unit distance graph*,  $G = (V, E)$ , of the triangular lattice. To show this, for any  $S_i$ , fix  $v_0 = 0 \cdot (1,0) + 0 \cdot \left( \frac{1}{2}, \frac{\sqrt{3}}{2} \right) = (0,0) \in V$  at origin. Next consider the six paths attached from origin. Fix each consecutive path  $\frac{\pi}{3}$  radians away from the next such that the following points like on the corresponding paths:  $(1,0) \in p_1, \left( \frac{1}{2}, \frac{\sqrt{3}}{2} \right) \in p_2, \left( -\frac{1}{2}, \frac{\sqrt{3}}{2} \right) \in p_3, (-1,0) \in p_4, \left( -\frac{1}{2}, -\frac{\sqrt{3}}{2} \right) \in p_5, \left( \frac{1}{2}, -\frac{\sqrt{3}}{2} \right) \in p_6$ . For  $S_i$ , there are  $i$  vertices on each path.

We define the six paths from origin as follows:

$$\begin{aligned} p_1 &= \{ a \cdot (1,0) = \vec{v} \mid a \in \mathbb{R}^+ \} \\ p_2 &= \left\{ a \cdot \left( \frac{1}{2}, \frac{\sqrt{3}}{2} \right) = \vec{v} \mid a \in \mathbb{R}^+ \right\} \\ p_3 &= \left\{ -a \cdot (1,0) + a \cdot \left( \frac{1}{2}, \frac{\sqrt{3}}{2} \right) = a \cdot \left( -\frac{1}{2}, \frac{\sqrt{3}}{2} \right) = \vec{v} \mid a \in \mathbb{R}^+ \right\} \\ p_4 &= \{ a \cdot (-1,0) = \vec{v} \mid a \in \mathbb{R}^+ \} \\ p_5 &= \left\{ a \cdot \left( -\frac{1}{2}, -\frac{\sqrt{3}}{2} \right) = \vec{v} \mid a \in \mathbb{R}^+ \right\} \\ p_6 &= \left\{ a \cdot (1,0) - a \cdot \left( \frac{1}{2}, \frac{\sqrt{3}}{2} \right) = a \cdot \left( \frac{1}{2}, -\frac{\sqrt{3}}{2} \right) \mid a \in \mathbb{R}^+ \right\} \end{aligned}$$

For  $S_i$  there exists  $i$  vertices on each path. We shall denote the  $i^{\text{th}}$  vertex on the  $j^{\text{th}}$  path as  $v_{j,i}$ . For each path defined above, the paths are defined as a set of vectors,  $\vec{v} = a \cdot \vec{p}$  for some  $a \in \mathbb{R}^+$  and  $\vec{p} \in \mathbb{R}^2$ . By setting  $a = 1, 2, \dots, i$ , we obtain points that are contained in  $V$ . For  $j = 1, 3, 5$  and  $l = 1, \dots, i$ , there exists two paths attached to each vertex  $v_{j,l}$ . For  $S_i$ , each path attached to the  $k^{\text{th}}$  vertex of  $p_j$ , there are  $i - k$  vertices. We will need to show that each of the  $i - k$  vertices on each corresponding path are also in  $V$ .

The triangular lattice is symmetice under rotation about  $v_0$  by  $\frac{\pi}{3}$  radians. For each vertex  $v_{1,l}$  for  $l = 1, 2, \dots, i - k$ , we place two paths from it; the first path  $\frac{\pi}{3}$  above  $p_1$  at  $v_{1,l}$  and  $-\frac{\pi}{3}$  below  $p_1$  at  $v_{1,l}$  and call these paths  $p_{1,l}^+$  and  $p_{1,l}^-$  respectively. With respect to  $v_{1,l}$ , one unit along  $p_{1,l}^+$  is a point on the triangular lattice and similarly so on  $p_{1,l}^-$ . Continuing the walk along these paths, unit distance-by-unit distance, we obtain the next point corresponding point on the the triangular lattice up to  $i - k$  distance away from  $v_{1,l}$ . This shows that each of the  $i - k$  vertices on  $p_{1,l}^-$  and  $p_{1,l}^+$  are in  $V$ . By rotating all of the paths along  $p_1$  by  $\frac{2\pi}{3}$  and  $\frac{4\pi}{3}$ , we obtain the the paths along  $p_3$  and  $p_5$  respectively, completing the construction.

**Perturbed Snowflake Tree.** The perturbed snowflake follows the construction of the perfect snowflake with the exception of  $v_0$  having weight  $\frac{1}{2} + \gamma$  where  $\gamma > 0$ . A perturbed snowflake realization has some distinct qualities from perfect snowflake realizations. The angular relationships between adjacent vertices

may vary; the distance between adjacent and neighboring vertices may vary as well. Note that we regard snowflakes with unit weight as a weight of  $\frac{1}{2}$ .

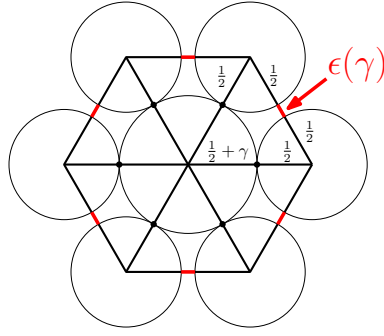


Figure 2.4: A canonical disk arrangement from a perturbed snowflake with 6 unit disks around a central disk with radius  $\frac{1}{2} + \gamma$ .

In Figure 2.4, we have a realization of disk arrangement from a perturbed snowflake. In a disk arrangement of a perfect snowflake, the disks around the central disk contact the adjacent disks. The disk arrangement from the perturbed snowflake does not have this quality. Figure 2.4 shows a gap  $\epsilon(\gamma)$  between adjacent disks around the central disk. This gap is formed from the perturbed weight  $\frac{1}{2} + \gamma$  of the central disk.

$$\epsilon(\gamma) = 2\gamma + \gamma^2 \quad (2.3)$$

**Lemma 6.** *Given any realization of a perturbed snowflake of 7 weighted vertices, with the central vertex  $v_0$  weighted  $\frac{1}{2} + \gamma$  and the others weighted  $\frac{1}{2}$ , the total additional distance between all vertices is  $6\epsilon(\gamma)$  compared to a perfect snowflake of 7 unit weight vertices.*

*As the perturbed snowflake grows outer layers, we can begin to define parts of the snowflake and the corresponding disk arrangement.*

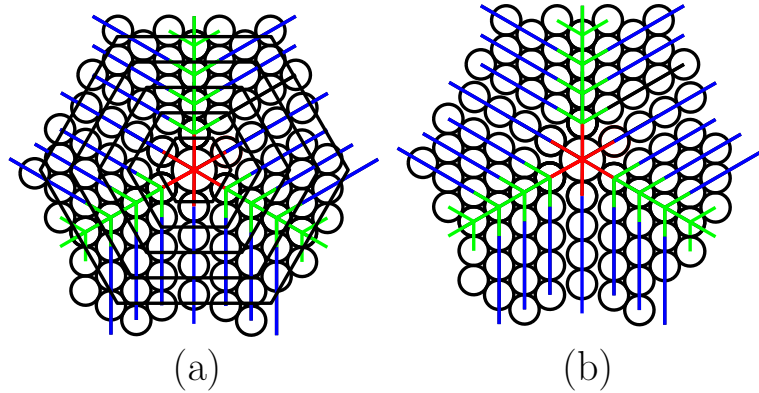


Figure 2.5

*In Figure 2.5, we show an overlay of a realization of a perturbed snowflake, a corresponding disk arrangement, and concentric hexagons about the  $v_0$ .*

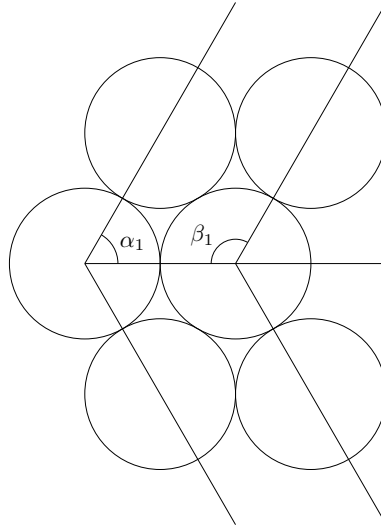


Figure 2.6: ?A?S

In Figure 2.6, we have a perturbed spine

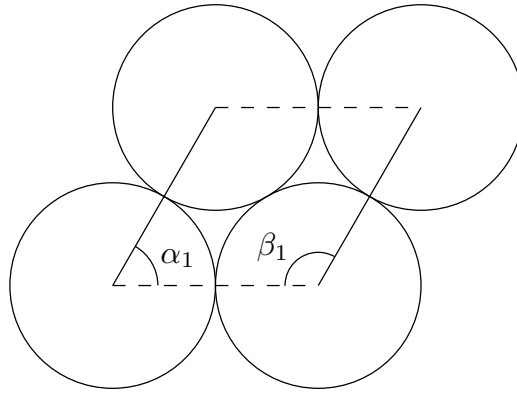


Figure 2.7: ?A?S

In Figure 2.7, we have four an arrangement of disks on the snowflake, off the spine and away from the central disk. We call this a vertebrae.

*Proof.* Consider a canonical disk arrangement of a perturbed snowflake of 7 weighted vertices (see Figure 2.4). The side length of the sides formed between the center of the central disk and two adjacent disks around the central disk is  $1 + \gamma$ . Let the distance between the two adjacent disks be  $1 + \varepsilon(\gamma)$ . There are a total of  $6\varepsilon(\gamma)$  between adjacent centers of disks. The total perimeter of the hexagon formed about the centers of the disks in contact with the central disk is  $6 + 6\varepsilon(\gamma)$ . Note that 1) the total perimeter of the hexagon formed on a perfect snowflake of 7 weighted vertices is 6 and 2) the canonical disk arrangement can be transformed to any other disk arrangement corresponding to the perturbed snowflake of 7 weighted vertices by pushing the the ring of disks around the central disk together such that all adjacent disks are in contact with each other with the exception of the disks at the end.  $\square$

### 2.3 On the Decidability of Problem ??

*Proof.* Consider a  $k \times (\sqrt{3}k)$  rectangle section of a triangular lattice, and place disks of radius 1 at each grid point as in Fig. ?????. The contact graph of these disks contains 2-cycles. Consider the spanning tree  $T$  of the contact graph indicated in Fig. ?????. The tree  $T$  decomposes into paths of collinear edges:  $T$  contains

two paths along the two main diagonals, each containing  $2k - 1$  vertices; all other paths have an endpoint on a main diagonal. We now modify the disk arrangement to ensure that its contact graph is  $T$ . The disks along the main diagonal do not change. We reduce the radii of all other disks by a factor of  $1 - k^{-3}$  (as a result, they lose contact with other disks), and then successively translate them parallel in the direction of the shortest path in  $T$  to the main diagonal until the contact with the adjacent disk is reestablished. The Hausdorff distance between the union of these disks and the initial  $k \times (\sqrt{3}k)$  rectangle is clearly less than 1. However, the contact tree  $T$  with these radii no longer has a unique realization (small perturbations are possible). To show stability, we argue by induction on the hop distance from the central disk. There are  $O(i)$  disks at  $i$  hops from the central disk, most one which have radius  $(1 - k^{-3})\frac{1}{2}$ . Since all radii are 1 or  $(1 - k^{-3})\frac{1}{2}$ , the six neighbors of the central disk can differ from the regular hexagon by at most  $O(k)$ . Similarly, the disks at  $i$  hops from the center be off from the triangular grid pattern by  $O(i2^{k-3})$ , for  $i = 1, 2, \dots, k$ .

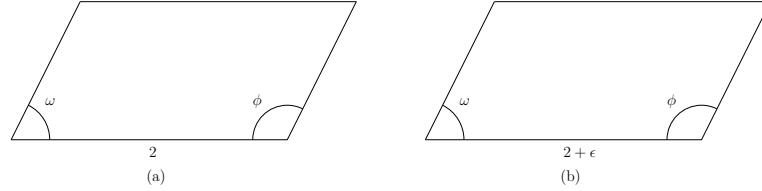


Figure 2.8

□

## Bibliography

- [1] James A Storer. On minimal-node-cost planar embeddings. *Networks*, 14(2):181–212, 1984.
- [2] R Tamassia and IG Tollis. Efficient embedding of planar graphs in linear time. In *Proc. IEEE Int. Symp. on Circuits and Systems*, pages 495–498, 1987.